Pyridine Degradation Intermediates as Models for Hydrodenitrogenation Catalysis: Preparation and Properties of a Metallapyridine Complex

Keith J. Weller,† Igor Filippov,‡ Paula M. Briggs, and David E. Wigley*

Carl S. Marvel Laboratories of Chemistry, Department of Chemistry, University of Arizona, Tucson, Arizona 85721-0041

Received August 21, 1997[⊗]

We report the preparation, structure, and reactions of a stable metallapyridine complex of tantalum prepared in the course of model studies of hydrodenitrogenation (HDN) reactions. Monomeric Ta(=NC^{t}Bu=CHC^{t}Bu=CH)(OAr)$_2$(THF) (**5**·THF) is isolated upon thermolyzing the $\eta^2(N,C)$-pyridine complex [$\eta^2(N,C)$-2,4,6-NC$_5$^{t}Bu$_3$H$_2$]Ta(OAr)$_2$Me (**2**) in the presence of THF, while the metallapyridine dimer [Ta(μ-NC^{t}Bu=CHC^{t}Bu=CH)(OAr)$_2$]$_2$ (**6**) is isolated when this reaction is carried out in benzene. Complete NMR characterization of **5**·THF is described, along with its conversion into **6**. The bis(pyridine) adduct Ta(=NC^{t}Bu=CHC^{t}Bu=CH)(OAr)$_2$(py)$_2$ (**5**·py) is also described. Ta(=NC^{t}Bu=CHC^{t}Bu=CH)(OAr)$_2$(THF) (**5**·THF) is shown to react with ^{t}BuNCO and ^{i}PrNCN^{i}Pr to afford the σ (η^1) and π (η^3) insertion products respectively Ta[=NC^{t}Bu=CHC^{t}Bu=CHC(=N^{t}Bu)O](OAr)$_2$ (**7**) and Ta[=NC^{t}Bu=CHC^{t}Bu=CH-(η^3-C(=N^{i}Pr)$_2$)](OAr)$_2$ (**8**). The molecular structure of the metallapyridine Ta(=NC^{t}Bu=CHC^{t}Bu=CH)(OAr)$_2$(THF) (**5**·THF) was detemined by X-ray crystallography and shown to adopt a trigonal-bipyramidal configuration with aryl oxide oxygens and the metallacyclic carbon occupying equatorial positions. The TaNC$_4$ metallacycle is very nearly planar, and discrete single and double bonds are evident around the ring. This π localization clearly favors the imido form Ta(=NC^{t}Bu=CHC^{t}Bu=CH)(OAr)$_2$(THF) rather than a carbene structure. The relevance of these compounds to hydrodenitrogenation catalysis is described.

Introduction

One major goal of petroleum hydrotreating is the catalytic removal of sulfur-, nitrogen-, oxygen-, and metal-containing impurities from assorted feedstocks.[1,2] Hydrotreating is typically carried out over sulfided CoMo/γ-Al$_2$O$_3$ or NiMo/γ-Al$_2$O$_3$ catalysts and is normally optimized for hydrodesulfurization (HDS), since sulfur is present in higher concentrations than nitrogen or oxygen.[3,4] However, declining crude oil quality is associated, in part, with increasing concentrations of organonitrogen contaminants, lending a new urgency to improving hydrodenitrogenation (HDN) technologies.[5,6] We recently described HDN model studies in which a pyridine C−N bond scission was achieved and led to a cascade of subsequent heterocycle rearrangement and degradation reactions.[7−10] In this report, we describe the isolation and structure of an elusive intermediate in this pyridine degradation sequence, *viz.* a monomeric metallapyridine complex. Various reactions of the metallapyridine are also described, including its conversion to the thermodynamic degradation product, a metallapyridine dimer. A portion of these results have been communicated.[10]

Results and Discussion

Synthesis and NMR Spectroscopy of a Metallapyridine Complex. The $\eta^2(N,C)$-pyridine complex [$\eta^2(N,C)$-2,4,6-NC$_5$^{t}Bu$_3$H$_2$]Ta(OAr)$_2$Cl (**1**, Ar = 2,6-C$_6$H$_3$-^{i}Pr$_2$) reacts with MeMgCl to ultimately afford a stable

† Present address: Witco Corp., OrganoSilicones Group, 777 Old Saw Mill River Rd., Tarrytown, NY 10591-6728.

‡ Link Foundation Energy Fellow, 1997−1998; Carl S. Marvel Fellow, 1997−1998.

⊗ Abstract published in *Advance ACS Abstracts,* December 15, 1997.

(1) Satterfield, C. N. *Heterogeneous Catalysis in Industrial Practice,* 2nd ed.; McGraw-Hill, Inc.: New York, 1991.

(2) Gary, J. H.; Handwerk, G. E. *Petroleum Refining: Technology and Economics,* 3rd ed.; Marcel Dekker, Inc.: New York, 1993.

(3) Ledoux, M. J. *Catalysis*; The Chemical Society: London, 1988; Vol. 7, pp 125−148.

(4) Angelici, R. J. In *Encyclopedia of Inorganic Chemistry*; King, R. B., Ed.; John Wiley and Sons: New York, 1994; Vol. 3, pp 1433−1443.

(5) Weller, K. J.; Fox, P. A.; Gray, S. D.; Wigley, D. E. *Polyhedron* **1997**, *16*, 3139.

(6) Ho, T. C. *Catal. Rev.-Sci. Eng.* **1988**, *30*, 117.

(7) Gray, S. D.; Smith, D. P.; Bruck, M. A.; Wigley, D. E. *J. Am. Chem. Soc.* **1992**, *114*, 5462.

(8) Gray, S. D.; Weller, K. J.; Bruck, M. A.; Briggs, P. M.; Wigley, D. E. *J. Am. Chem. Soc.* **1995**, *117*, 10678.

(9) Weller, K. J.; Gray, S. D.; Briggs, P. M.; Wigley, D. E. *Organometallics* **1995**, *14*, 5588.

(10) Weller, K. J.; Filippov, I.; Briggs, P. M.; Wigley, D. E. *J. Organomet. Chem.* **1997**, *528*, 225.

S0276-7333(97)00749-8 CCC: $15.00
Publication on Web 01/16/1998

Scheme 1

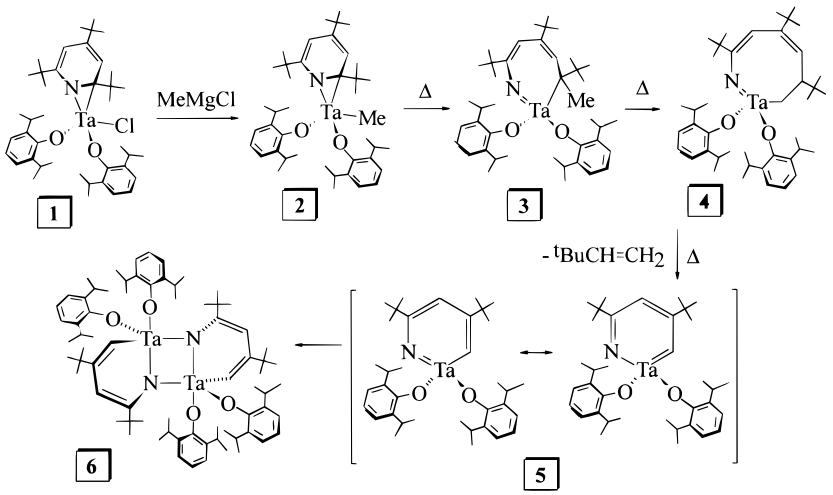

metallapyridine dimer, [Ta(μ-NC^{t}Bu=CHC^{t}Bu=CH)(OAr)$_2$]$_2$ (**6**), Scheme 1.[8] The initial kinetic product in this sequence, [η^2(*N*,*C*)-2,4,6-NC$_5$^{t}Bu$_3$H$_2$]Ta(OAr)$_2$Me (**2**), has been shown to undergo an intramolecular metal-to-ligand alkyl migration[9] that induces pyridine ring opening and forms the metallacyclic imido complex Ta(=NC^{t}Bu=CHC^{t}Bu=CHC^{t}BuMe)(OAr)$_2$ (**3**). Further studies of metallacycle **3** revealed its instability with respect to "ring expansion" to afford Ta(=NC^{t}Bu=CHC^{t}Bu=CHC^{t}BuHCH$_2$)(OAr)$_2$ (**4**) that further decomposes to give the metallapyridine dimer [Ta(μ-NC^{t}Bu=CHC^{t}Bu=CH)(OAr)$_2$]$_2$ (**6**) and ^{t}BuCH=CH$_2$, when the thermolysis is effected in benzene solution, Scheme 1.[8]

With the exception of **5**, all of the complexes in Scheme 1 have been observed *via* ^{1}H and ^{13}C NMR spectroscopy, **1**−**3** and **6** have been isolated as the complexes shown, and **4** has been isolated as its MeC≡N adduct.[8] We believed that complex **6** is formed from the dimerization of monomeric metallapyridine **5**, which is sufficiently short-lived in solution that it is not observed. We have now succeeded in isolating an adduct of **5** and describe its structure, characterization, and reactivity.

Thermolyzing toluene/THF solutions of [η^2(*N*,*C*)-2,4,6-NC$_5$^{t}Bu$_3$H$_2$]Ta(OAr)$_2$Me (**2**) affords a new, cherry-red species that can be isolated in moderate yield from concentrated pentane solutions. The ^{1}H NMR spectrum of this red complex reveals two sharp singlets at δ 7.41 and 5.97 for the ring protons as compared to a broad singlet at δ 5.63 for the pyridine protons of **2** that are equilibrating by a "ring-rocking" process (all in C$_6$D$_6$).[8,11] This new compound is also characterized by only *two* ^{t}Bu resonances in its ^{1}H NMR spectrum, along with signals for a coordinated THF. Based upon its ^{1}H and ^{13}C NMR spectra, as well as its elemental analysis, this new complex is formulated as the metallapyridine monomer Ta(NC^{t}BuCHC^{t}BuCH)(OAr)$_2$(THF), **5**·THF. The monomer can also be isolated as a bis(pyridine) adduct (**5**·py) by recrystallizing **5**·THF from concentrated pentane solutions with the addition of a small amount of pyridine.

There are two isomers of **5**·THF, both C_s-symmetric, that are consistent with the ^{1}H and ^{13}C NMR data. Both structures **5a**,**b** are trigonal bipyramids with the coordinated THF assuming an apical position and the aryl oxide ligands occupying equatorial sites. The metallapyridine ring itself can be oriented such that the imido nitrogen is either *trans* to the THF ligand (as in **5a**) or *cis* to the THF (as in **5b**). Structure **5a** appears to be preferred since L→M π donation is maximized in this arrangement. If the *z*-axis lies along the Ta−N bond and the *x*-axis is coincident with the Ta−C bond in **5a**, then the aryl oxide oxygens interact with the d_{xy} orbital, while the imido nitrogen π donates into d_{xz} and d_{yz}. In **5b**, however, both aryl oxide oxygens and the imido nitrogen compete for donation into the d_{xy} orbital, suggesting that **5b** is less favorable.

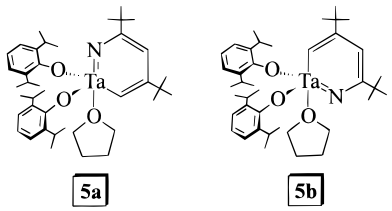

In order to determine which structure **5**·THF adopts in solution, as well as to make complete NMR assignments, a NOESY experiment was carried out. The numbering scheme for **5**·THF carbon nuclei used in specifying ^{1}H and ^{13}C NMR assignments is shown in Figure 1. NOE cross-peaks were observed between the resonance at δ 5.97 and both ^{t}Bu groups (at δ 1.34 and 0.95), establishing the δ 5.97 resonance as C3H. NOE cross-peaks also appeared between the δ 7.41 ring proton and only one ^{t}Bu resonance (δ 1.34), as well as the THF CαH resonance at δ 3.89. Based upon these observations, the structure of **5**·THF can be assigned as that of **5a**, with the C1H and C3H resonances assigned at δ 7.41 and 5.97, respectively. The ^{t}Bu groups can also be assigned, with C6H and C8H signals assigned at δ 1.34 and 0.97, respectively. A summary

(11) At −90 °C in toluene-d_8, the "ring-rocking" process that equilibrates the ring protons in [η^2(*N*,*C*)-2,4,6-NC$_5$^{t}Bu$_3$H$_2$]Ta(OAr)$_2$Me (**2**) is slowed, and their resonances in a static pyridine ligand appear at δ 5.73 and 5.50.

Table 1. Summary of ^{1}H NMR Data for Complexes Ta(=NC^{t}Bu=CHC^{t}Bu=CH)(OAr)$_2$(THF) (5·THF), Ta(=NC^{t}Bu=CHC^{t}Bu=CH)(OAr)$_2$(py)$_2$ (5·py), Ta[=NC^{t}Bu=CHC^{t}Bu=CHC(=N^{t}Bu)O](OAr)$_2$ (7), and Ta[=NC^{t}Bu=CHC^{t}Bu=CH(η^3-C(=N^{i}Pr)$_2$)](OAr)$_2$ (8)[a]

	compound			compound	
assignment	**5**·THF	**5**·py	assignment	**7**	**8**
C1H	7.41	7.46	C2H	6.61 d, $^4J_{HH}$ = 1.3 Hz	5.61 d, $^4J_{HH}$ = 0.7 Hz
C3H	5.97	5.99	C4H	6.71 d, $^4J_{HH}$ = 1.3 Hz	5.24 d, $^4J_{HH}$ = 0.7 Hz
C6H	1.34	1.28	C9H	1.07	1.09
C8H	0.97	1.03	C11H	1.36	1.32
			C6H		4.12 spt
			C7H	1.51 (CMe_3)	1.16 d, 1.06 d
C*H*Me$_2$	3.74 spt	3.79 spt	C*H*Me$_2$	3.67 spt	3.96 spt
CH*Me*$_2$	1.36 d, 1.34 d	1.32 d, 1.29 d	CH*Me*$_2$	1.26 d, 1.18 d	1.36 d, 1.29 d
L (THF or py)	3.89 m, 1.19 m (THF)	8.71, 6.83 t, 6.52 t (py)			
aryl region	7.20 A$_2$B d, 6.99 A$_2$B t	7.23 A$_2$B d, 7.02 A$_2$B t	aryl region	7.10 A$_2$B d, 6.95 A$_2$B t	7.14 A$_2$B d, 6.96 A$_2$B t

[a] Reported in δ in C_6D_6 at probe temperature.

Table 2. Summary of ^{13}C NMR Data for Complexes Ta(=NC^{t}Bu=CHC^{t}Bu=CH)(OAr)$_2$(THF) (5·THF), Ta(=NC^{t}Bu=CHC^{t}Bu=CH)(OAr)$_2$(py)$_2$ (5·py), Ta[=NC^{t}Bu=CHC^{t}Bu=CHC(=N^{t}Bu)O](OAr)$_2$ (7), and Ta[=NC^{t}Bu=CHC^{t}Bu=CH(η^3-C(=N^{i}Pr)$_2$)](OAr)$_2$ (8)[a]

	compound			compound	
assignment	**5**·THF	**5**·py	assignment	**7**	**8**
			C1	163.6	165.3
C1	178.5	181.6	C2	104.0	106.4
C2	172.4	171.2	C3	164.9	150.2
C3	121.4	121.5	C4	107.8	113.4
C4	167.8	167.5	C5	167.5	167.9
C5, C7	37.9, 36.7	37.9, 36.7	C6, C8, C10	55.7, 37.6, 35.3	50.4, 40.2, 38.8
C6, C8	31.4, 29.1	31.4, 29.1	C7, C9, C11	30.9, 30.3, 30.2	24.9,[c] 22.9,[c] 30.1[d]
CH*Me*$_2$ OAr	24.1, 23.9	24.16, 24.0	CH*Me*$_2$ OAr	24.0, 23.9	24.0, 23.7
C*H*Me$_2$ OAr	27.2	27.2	C*H*Me$_2$ OAr	27.1	27.1
L (THF or py)	71.6, 25.4 (THF)	149.9, 124.1 (py)[b]			
C$_{ipso}$ OAr	160.0	160.1	C$_{ipso}$ OAr	157.2	157.2
C$_{ortho}$ OAr	136.7	136.9	C$_{ortho}$ OAr	137.8	138.2
C$_{meta}$ OAr	123.3	123.4	C$_{meta}$ OAr	123.7	123.5
C$_{para}$ OAr	121.6	121.7	C$_{para}$ OAr	122.8	122.6

[a] Reported in δ in C_6D_6 at probe temperature. [b] One resonance for pyridine could not be found and is presumably coincident with an aryl resonance. [c] Resonances for C7 and C7′. [d] C9 and C11 are coincident at 30.1 ppm.

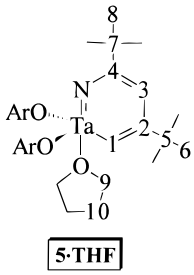

5·THF

Figure 1. Numbering scheme for Ta(=NC^{t}Bu=CHC^{t}Bu=CH)(OAr)$_2$(THF) (**5**·THF) carbon nuclei used in specifying ^{1}H and ^{13}C NMR assignments.

of ^{1}H NMR data for **5**·THF and other complexes reported here are presented in Table 1.

With the exception of C2 and C4, the ^{13}C NMR spectrum is also completely assigned based upon these NOESY data and a HETCOR experiment. In the interest of making a complete spectral assignment for comparisons (*vide infra*), a heteronuclear multiple-bond correlation (HMBC) experiment, which can provide assignment information for nonprotonated carbons via $^2J_{CH}$ and $^3J_{CH}$ couplings, was also carried out.[12] Based upon the data from all of these experiments, the ring carbons can now be conclusively assigned. Thus, C1 appears farthest downfield at δ 178.5, C2 and C4 appear at δ 172.5 and 167.8, respectively, and C3 occurs at δ 121.4 (C_6D_6). A summary of ^{13}C NMR data for **5**·THF and other compounds prepared in this study are presented in Table 2, and selected NMR correlation data for **5**·THF are provided in Table 3 based upon the numbering scheme in Figure 1.

Table 3. Summary of Observed NMR Connectivities for Ta(=NC^{t}Bu=CHC^{t}Bu=CH)(OAr)$_2$(THF) (5·THF) with NOESY, HETCOR, and HMBC Methods

^{1}H signal	NOESY (^{1}H)	HETCOR (^{13}C)	HMBC (^{13}C)
C1H	C9H, C6H	C1	C2, C3, C5
C3H	C6H, C8H	C3	C1, C2, C4, C5, C7
C6H	C1H, C3H	C6	C2, C5, C6
C8H	C3H	C8	C4, C7, C8
C9H	C1H, C10H	C9	
C10H	C9H	C10	

Structural Study of Ta(NC^{t}BuCHC^{t}BuCH)(OAr)$_2$(THF) (5·THF). One significant structural question concerning metallapyridine **5**·THF is the extent to which the metallacycle is delocalized.[13] We have pre-

(12) Summers, M. F.; Marzilli, L. G.; Box, A. *J. Am. Chem. Soc.* **1986**, *108*, 4285.
(13) Bleeke, J. R. *Acc. Chem. Res.* **1991**, *24*, 271.

Table 4. Details of the X-ray Diffraction Studies for Ta(=NC^{t}Bu=CHC^{t}Bu=CH)(OAr)$_2$(THF) (5·THF)

Crystal Parameters	
mol formula	$C_{40}H_{62}NO_3Ta$
mol wt	785.89
F(000)	1624
cryst color	orange
space group	triclinic $P\bar{1}$ (No. 2)
unit cell volume, Å^3	4013.5(9)
a, Å	13.397(2)
b, Å	16.925(2)
c, Å	19.531(1)
α, deg	108.06(1)
β, deg	103.11(1)
γ, deg	96.86(1)
Z	4
D(calcd), g cm^{-3}	1.30
cryst dimens, mm	0.33 × 0.33 × 0.08
ω width, deg	0.40
abs coeff, cm^{-1}	27.4
data collection temp, °C	−70 ± 1
Data Collection	
diffractometer	Enraf-Nonius CAD4
monochromator	graphite crystal, incident beam
attenuator	Zr foil, factor 13.5
Mo Kα radiation, λ, Å	0.71073
2θ range, deg	2−50
octants collected	$+h, \pm k, \pm l$
scan type	$\omega - 2\theta$
scan speed, deg min^{-1}	0−20 (in ω)
scan width, deg	0.8 + 0.340 tan θ
total no. of reflns measd	14739 (14075 unique)
corrections	Lorentz polarization reflection averaging (agreement on I = 9.8%) ψ-scan absorption (min 0.589, max 0.999, av 0.872)
Solution and Refinement	
solution	Patterson heavy-atom method
refinement	full-matrix least-squares
minimization function	$\sum w(\|F_o\| - \|F_c\|)^2$
no. of reflns used in refinement, $I > 3\sigma(I)$	7928
no. of params refined	806
$R(\sum\|\|F_o\| - \|F_c\|/\sum\|F_o\|)$	0.052
$R_w([\sum w(\|F_o\| - \|F_c\|)^2/\sum w(F_o)^2]^{1/2})$	0.056
esd of obsd of unit weight	1.29
convergence, largest shift	0.28σ
Δ/σ(max), e^{-1}/Å^3	3.02(17)
Δ/σ(min), e^{-1}/Å^3	−0.22(17)
computer hardware	VAX
computer software	MolEN, 1990

sented the structure of **5**·THF as an imido complex in Figure 1, but a carbene structure of **5** (shown in Scheme 1) or a delocalized form is also a possible alternative.

The assignment and structure of **5**·THF as a metallapyridine monomer, Ta(NC^{t}BuCHC^{t}BuCH)(OAr)$_2$(THF), was confirmed by an X-ray crystallographic study. Dark-orange, almost red, single crystals of **5**·THF suitable for a structural study were grown from a concentrated pentane solution at −35 °C. **5**·THF crystallizes in the triclinic space group $P\bar{1}$ with the asymmetric unit containing two crystallographically independent, but virtually identical, molecules. Tables 4 and 5 present details of the crystallographic study and important metrical parameters of molecule 1 of **5**·THF, a full ORTEP drawing of molecule 1 is shown in Figure 2, and a core structure is presented in Figure 3. Complex **5**·THF adopts a slightly distorted trigonal-bipyramidal configuration with the aryl oxide oxygens

Table 5. Selected Bond Distances (Å) and Bond Angles (deg) in Molecule 1 of Ta(=NC^{t}Bu=CHC^{t}Bu=CH)(OAr)$_2$(THF) (5·THF)[a]

Bond Distances			
Ta−N	1.786(9)	C(2)−C(3)	1.45(2)
Ta−C(1)	2.15(1)	C(3)−C(4)	1.36(2)
Ta−O(10)	1.924(8)	C(4)−N	1.34(1)
Ta−O(20)	1.934(8)	O(10)−C(11)	1.38(1)
Ta−O(30)	2.249(7)	O(20)−C(21)	1.35(1)
C(1)−C(2)	1.35(2)		
Bond Angles			
Ta−N−C(4)	148.0(8)	C(1)−Ta−O(10)	112.8(4)
Ta−C(1)−C(2)	127.7(9)	C(1)−Ta−O(20)	115.8(4)
Ta−O(10)−C(11)	140.2(7)	O(10)−Ta−O(20)	128.1(3)
Ta−O(20)−C(21)	132.7(7)	C(1)−C(2)−C(3)	123(1)
N−Ta−C(1)	80.6(4)	C(2)−C(3)−C(4)	124(1)
N−Ta−O(10)	104.5(4)	N−C(4)−C(3)	117(1)
N−Ta−O(20)	100.1(4)		

[a] Numbers in parentheses are estimated standard deviations in the least significant digits.

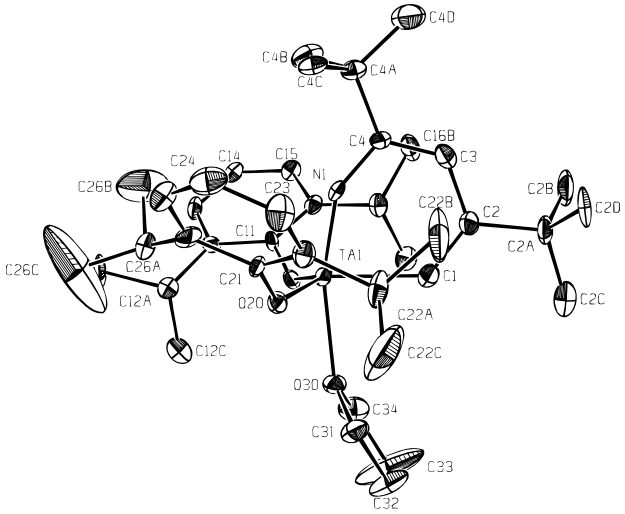

Figure 2. ORTEP drawing of Ta(=NC^{t}Bu=CHC^{t}Bu=CH)(OAr)$_2$(THF) (**5**·THF), with atoms shown as 50% probability ellipsoids.

and metallacyclic C1 occupying equatorial positions, in agreement with the solution structure; the THF ligand and metallacyclic nitrogen occupy axial positions. The aryl oxide ligands are folded upward toward the ring with one isopropyl substituent from each ligand positioned over opposite faces of the metallacycle ring to provide a protective cleft for the ring and the metallapyridine nitrogen. The $TaNC_4$ ring itself is very nearly planar (mean deviation from planarity = 0.02 Å), but *it is not delocalized*, as discrete single and double bonds are evident around the ring. This π electron localization clearly favors the imido form Ta(=NC^{t}Bu=CHC^{t}Bu=CH)(OAr)$_2$(THF) rather than a carbene structure, which is especially significant since the metal can dictate that either arrangement be adopted. Although the imido ligand in **5**·THF is strongly bent [Ta=N−C(4) = 148.0(8)°], it is only weakly basic as attempts to alkylate the imido nitrogen with electrophiles were unsuccessful (*vide infra*).

We believe the stability of **5**·THF with respect to dimerization arises from the protection of the imido nitrogen afforded by the aryl oxide ligands in a five-

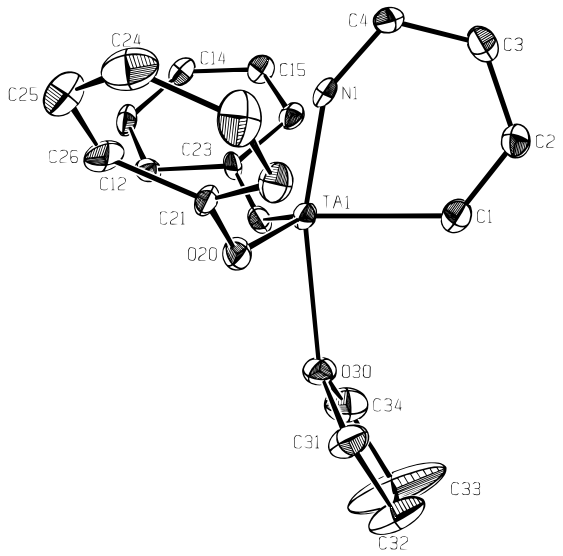

Figure 3. ORTEP drawing of the core structure of Ta(=NC^{t}Bu=CHC^{t}Bu=CH)(OAr)$_2$(THF) (**5**·THF), with atoms shown as 50% probability ellipsoids.

Scheme 2

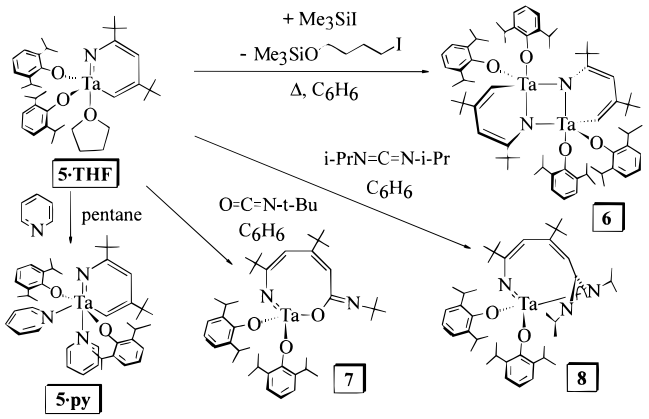

coordinate structure. Generating base-free **5** in the absence of THF provides a less-congested, four-coordinate structure that cannot be isolated, but which rapidly dimerizes to form **6**.

Reactivity of Metallapyridine Ta(=NC^{t}Bu=CHC^{t}Bu=CH)(OAr)$_2$(THF) (5·THF). When a concentrated pentane/pyridine solution of **5**·THF is cooled to −35 °C for several hours, red samples of the bis(pyridine) adduct Ta(=NC^{t}Bu=CHC^{t}Bu=CH)(OAr)$_2$(py)$_2$ (**5**·py) can be isolated in good yield, Scheme 2. The ^{1}H and ^{13}C NMR spectra of **5**·py reveal equivalent pyridine ligands on the NMR time scale, suggesting a rapid equilibrium involving the dissociation of one pyridine ligand, *i.e.*, Ta(=NC^{t}Bu=CHC^{t}Bu=CH)(OAr)$_2$(py)$_2$ ⇄ Ta(=NC^{t}Bu=CHC^{t}Bu=CH)(OAr)$_2$(py) + py. Note that a static, C_s-symmetric, six-coordinate solution structure with *trans*-pyridine ligands is ruled out on the basis of the *equivalent* aryl oxide ligands observed by ^{1}H and ^{13}C NMR. Pyridine exchange is confirmed by the single pyridine environment observed in the ^{1}H NMR spectrum of solutions of **5**·py in which free pyridine has been added (C_6D_6, 300 MHz). One possible solid-state structure of **5**·py is presented in Scheme 2.

Although base-free **5** is not observed by ^{1}H NMR spectroscopy during the thermal conversion of **2** to dimer **6** (Scheme 1), its intermediacy is supported by the fact that Ta(=NC^{t}Bu=CHC^{t}Bu=CH)(OAr)$_2$(THF) (**5**·THF) can be cleanly converted into **6**. Heating a cherry-red solution of **5**·THF with Me_3SiI results in the decolorization of the solution and the formation of insoluble red crystals, Scheme 2. The only product observed in solution by ^{1}H NMR is $Me_3SiOCH_2CH_2CH_2CH_2I$, which arises from ring cleavage of the THF ligand of **5**·THF.[14] The insoluble red crystals were identified as dimer **6** by elemental analysis and by comparison of one crystal's unit cell parameters to those of an authentic sample of **6**.[8]

Complex **5**·THF also reacts at room temperature with electrophiles such as isocyanates and carbodiimides to afford insertion products. Thus, reacting **5**·THF with ^{t}BuNCO (C_6H_6 solution) provides a metallacyclic insertion product formulated as Ta[=NC^{t}Bu=CHC^{t}Bu=CHC(=N^{t}Bu)O](OAr)$_2$ (**7**), shown in Scheme 2. This σ (η^1) insertion complex contrasts with the proposed π (η^3) insertion species formed upon reacting **5**·THF with ^{i}PrNCN^{i}Pr, *viz.* Ta[=NC^{t}Bu=CHC^{t}Bu=CH(η^3-C(=N^{i}Pr)$_2$)](OAr)$_2$ (**8**), Scheme 2. This structural formulation of **8** is proposed on the basis of the equivalent ^{i}Pr groups of the inserted ^{i}PrNCN^{i}Pr moiety, indicating a complex with a molecular plane of symmetry. Although this observation is also consistent with a rapid equilibrium between two $\sigma(\eta^1)$ insertion isomers (eq 1), this process does not appear to be operative as judged by low-temperature ^{1}H NMR studies of **8** (toluene, −90 °C) in which this equivalence is maintained.

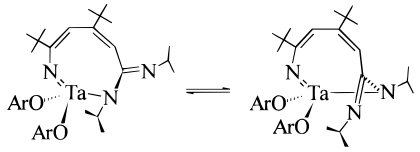

The ^{1}H and ^{13}C NMR data of **7** and **8** are summarized in Tables 1 and 2. Their formulations were assisted by HETCOR and HMBC experiments, and the observed connectivities from these methods are presented in Table 6, based upon the numbering schemes shown in Figure 4. The spectrum of **7** is very similar to that of **5**·THF without the THF resonances; the ring protons in **7** appear at δ 6.71 and 6.61 as doublets ($^4J_{HH}$ = 1.3 Hz, C_6D_6), and there are now three ^{t}Bu resonances for the metallacycle. The HMBC experiment proved to be invaluable for the conclusive assignment of **7** as an eight-membered ring complex, Table 6. The HETCOR experiment gave assignments for the ring protons C2H and C4H as well as for the ^{t}Bu groups and provided a convenient starting point for the assignment of the HMBC data.

Based upon the HMBC data, the resonance at δ 6.61 in the ^{1}H NMR spectrum of **7** can be identified as C2H, since it is coupled to C1, C4, and C8. Similarly, the

(14) van der Heijden, H.; Schaverien, C. J.; Orpen, A. G. *Organometallics* **1989**, *8*, 255.

Table 6. Summary of Observed NMR Connectivities for Ta[=NC^{t}Bu=CHC^{t}Bu=CHC(=N^{t}Bu)O](OAr)$_2$ (7) and Ta[=NC^{t}Bu=CHC^{t}Bu=CH(η^3-C(=N^{i}Pr)$_2$)](OAr)$_2$ (8) with HETCOR and HMBC Methods

^{1}H signal	HETCOR (^{13}C)	HMBC (^{13}C)
Ta[=NC^{t}Bu=CHC^{t}Bu=CHC(=N^{t}Bu)O](OAr)$_2$ (**7**)		
C2H	C2	C1, C4, C8[a]
C4H	C4	C2, C5, C8, C10[a]
C7H	C7	C6
C9H	C9	C3, C8
C11H	C11	C5, C10
Ta[=NC^{t}Bu=CHC^{t}Bu=CH(η^3-C(=N^{i}Pr)$_2$)](OAr)$_2$ (**8**)		
C2H	C2	C1, C3, C4, C8
C4H	C4	C2, C8, C10[b]
C6H	C6	C1, C7
C7H	C7	C6
C9H	C9	C3, C8
C11H	C11	C5, C10

[a] Cross-peak was not observed to C3. [b] Cross-peaks were not observed to C3 or C5.

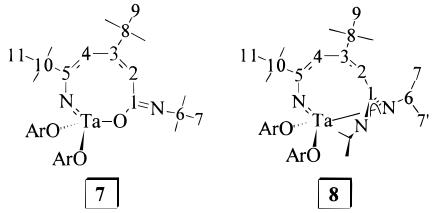

Figure 4. Numbering scheme for Ta[=NC^{t}Bu=CHC^{t}Bu=CHC(=N^{t}Bu)O](OAr)$_2$ (**7**) and Ta[=NC^{t}Bu=CHC^{t}Bu=CH(η^3-C(=N^{i}Pr)$_2$)](OAr)$_2$ (**8**) carbon nuclei used in specifying ^{1}H and ^{13}C NMR assignments.

resonance at δ 6.71 can be identified as C4H by its coupling with C2, C5, C8, and C10. Although no coupling from either C2H or C4H to C3 is observed, both C2H and C4H are coupled through C3 to C8 and C9H is coupled to C3. With the central ^{t}Bu group of the ring identified, the other two ^{t}Bu groups can now be assigned, since C11H is coupled to both C10 and C5 while C7H is only coupled to C6, being attached to the nitrogen derived from the isocyanate. Finally, we note that these data do not distinguish between the Ta−O-bonded η^1 insertion product indicated in Scheme 2 and a Ta−N-bonded insertion species of the form Ta[=NC^{t}Bu=CHC^{t}Bu=CHC(=O)N^{t}Bu](OAr)$_2$. However, the greater steric restrictions of the Ta−N σ insertion derivative argues for the structure indicated in Scheme 2. Similar NMR assignments for complex **8** were made on the basis of HETCOR and HMBC experiments.

We note that although metal imido functionalities are well-known to engage in cycloaddition reactions with isocyanates and carbodiimides,[15] these reagents both insert at the Ta−C bond rather than at the Ta−N imido linkage. These insertions into a d^0 metal−carbon bond are analogous to the reverse of the olefin elimination reaction in metallacycle **4**, providing further support for the intermediacy of **5** as shown in Scheme 1.

Although the imido moiety in **5**·THF is strongly bent, it appears to be only very weakly basic as attempts to alkylate the imido nitrogen with electrophiles such as MeI were unsuccessful. Reacting **5**·THF with carbon dioxide failed to provide any isolable products. Attempts to perform insertion reactions of **5**·THF with 2-butyne (C_6D_6, 80 °C, 10 min) afforded no isolable organometallic species; however, the principal product identified from this reaction (^{1}H NMR and GC/mass spectrometry) is 1,5-di-*tert*-butyl-2,3-dimethylbenzene, Scheme 3. Similarly, the reactions of **5**·THF with ^{t}BuC≡CH and ^{t}BuC≡N (C_6D_6, 80 °C, 1 h) afforded no isolable organometallics, but 1,3,5-tri-*tert*-butylbenzene and 2,4,6-tri-*tert*-butylpyridine, respectively, were major products, Scheme 3. These intriguing results suggest a Diels−Alder addition into the diene portion of Ta(=NC^{t}Bu=CHC^{t}Bu=CH)(OAr)$_2$(THF) (**5**·THF) to generate these organic products. The metal-containing byproduct in both of these reactions is nominally the nitride species [Ta(N)(OAr)$_2$]$_n$; however, we have been unable to trap such a species when these reactions are carried out in the presence of Lewis bases.

Scheme 3

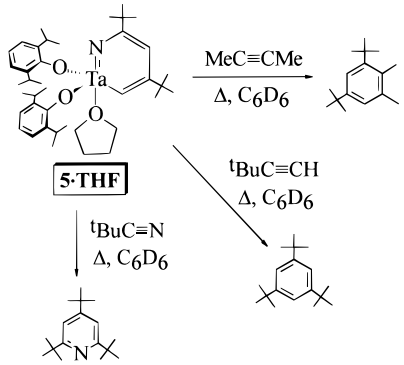

Discussion

Although metallabenzenes such as (Et$_3$P)$_3$Ir(CHCMeCHCMeCH) have been prepared and structurally characterized as *delocalized*,[13,16] metallapyridine **5**·THF is significant in favoring the *localized* imido form Ta(=NC^{t}Bu=CHC^{t}Bu=CH)(OAr)$_2$(THF) rather than a delocalized or carbene structure, even though the metallabenzene ring is planar. In addition, the ^{1}H and ^{13}C NMR chemical shifts of **5**·THF and its Diels−Alder reactivity are indicative of a localized diene structure, again in contrast to Bleeke's iridabenzene (Et$_3$P)$_3$Ir(CHCMeCHCMeCH).[13,16]

We have demonstrated the formation of a monomeric metallapyridine complex (**5**·THF) from thermolysis of the $\eta^2(N,C)$-pyridine complex [$\eta^2(N,C)$-2,4,6-NC$_5$-^{t}Bu$_3$H$_2$]Ta(OAr)$_2$Me (**2**) in the presence of THF. Nascent Ta(NC^{t}BuCHC^{t}BuCH)(OAr)$_2$ (**5**) is generated by removal of a THF ligand from **5**·THF, and its conversion into dimeric [Ta(μ-NC^{t}Bu=CHC^{t}Bu=CH)(OAr)$_2$]$_2$ (**6**) has been established. These observations complete the

(15) Wigley, D. E. *Prog. Inorg. Chem.* **1994**, *42*, 239.

(16) Bleeke, J. R.; Xie, Y.-F.; Peng, W.-J.; Chiang, M. *J. Am. Chem. Soc.* **1989**, *111*, 4118.

reaction sequence in Scheme 1, delineate one process by which heterocyclic C−N bonds are cleaved, and offer additional insight into how nitrogen heterocycles may be further degraded *after* C−N bond cleavage. Thus, in cases where a highly substituted metallacycle arises from pyridine ring opening, subsequent heterocycle degradation pathways exist. This information may be relevant to catalytic HDN since under normal HDN conditions ethane, ethylene, propane, and propylene are the principal products of pyridine HDN with only a *minor fraction* of C_5 products being generated.[17] We note that Wolczanski and co-workers have uncovered very different mechanisms by which C−N bonds may be cleaved in nitrogen heterocycles[18] and anilines.[19]

In the metallaaziridine description of complex **2**,[20,21] the C−N scission reaction in Scheme 1 transforms a formal *amido* nitrogen in the $\eta^2(N,C)$-pyridine to a formal *imido* nitrogen in the ring-opened structure. This reaction appears to be driven largely by the formation of a strong metal−ligand multiple bond in **3**. It now seems likely that this strong Ta=N bond is maintained through compounds **4** and **5** (neither **4** nor base-free **5** is structurally characterized) until dimerization to form **6** occurs. In this system, tantalum nitrido species may constitute the ultimate fate of the pyridine nitrogen. Studies of these processes are continuing.

Experimental Section

General Details. All manipulations were performed under a nitrogen atmosphere either by standard Schlenk techniques[22] or in a Vacuum Atmospheres HE-493 drybox at room temperature (unless otherwise indicated). Solvents were distilled under N_2 from an appropriate drying agent[23] and were transferred to the drybox without exposure to air. NMR solvents were passed down a short (5−6 cm) column of activated alumina prior to use. Thermolyses were typically conducted in sealed NMR tubes in an oil bath maintained at the specified temperature. In all preparations Ar = 2,6-C_6H_3-^{i}Pr$_2$.

Starting Materials. $[\eta^2(N,C)$-2,4,6-$NC_5{}^t Bu_3H_2]Ta(OAr)_2$Me (**2**) was prepared from $[\eta^2(N,C)$-2,4,6-$NC_5{}^t Bu_3H_2]Ta(OAr)_2$Cl (**1**) as previously described.[8] Trimethylsilyl iodide, methyl iodide, and diisopropylcarbodiimide were obtained from Aldrich and used as received. Isocyanate ^{t}BuNCO was obtained from Aldrich and distilled prior to use. Carbon dioxide was purified by passage through a column of activated 4-Å molecular sieves and activated Ridox catalyst (supported Cu) prior to use.

Physical Measurements. ^{1}H (250 and 300 MHz) and ^{13}C (62.9 and 75.4 MHz) NMR spectra were recorded at probe temperature (unless otherwise specified) on a Bruker AM-250 or Varian Unity 300 spectrometer in C_6D_6 solvent. Chemical shifts are referenced to protio impurities (δ 7.15) or solvent ^{13}C resonances (δ 128.0) and are reported downfield of Me_4Si. Spectral assignments are based upon the ring numbering systems indicated in Figures 1 and 4. All 2D spectra were acquired at 25 °C without spinning the sample. NOESY and natural abundance {^{13}C−^{1}H} heteronuclear multiple-bond correlation (HMBC) spectra[12] were acquired in the phase-sensitive mode using time-proportional phase incrementation (TPPI). The NOESY spectrum resulted from a 1024 × 4096 data matrix with 8 scans per t_1 value. The delay time between scans was 1 s, and the total measurement time was 9.2 h. The HMBC spectra resulted from 512 × 2048 data matrices with 16 scans per t_1 value and a delay time between scans of 1 s. The delay to allow long-range heteronuclear antiphase magnetization to develop for multiple-bond correlations was 60 ms. The total acquisition time was 4.1 h/spectrum. The HETCOR spectrum resulted from a 512 × 4096 data matrix with 16 scans per t_1 value. The delay time between scans was 1 s, and the total measurement time was 3.2 h. Infrared spectra were recorded on a Nicolet 510P FTIR spectrometer in C_6H_6 solutions in a sealed CsI cell and were used as fingerprints. Electron ionization mass spectra (70 eV) were recorded to m/z = 999 on a Hewlett Packard 5970 mass selective detector and RTE-6/VM data system. For GC/mass spectra, the sample was introduced into the mass spectrometer by a Hewlett Packard model 5890 gas chromatograph equipped with an HP-5 column. Microanalytical samples were handled under nitrogen and were combusted with WO_3 (Desert Analytics, Tucson, AZ).

Preparations. Ta(=NC^{t}Bu=CHC^{t}Bu=CH)(OAr)$_2$(THF) (5·THF). An ampule (Teflon stopcock) was charged with $[\eta^2(N,C)$-2,4,6-$NC_5{}^t Bu_3H_2]Ta(OAr)_2$Me (450 mg, 0.564 mmol), 8 mL of toluene, and 450 μL of THF. The stopcock was sealed, and the resulting orange solution was heated in an oil bath maintained at 110 °C for 4 days, over which time the solution developed a cherry-red color. The solution was allowed to cool, the reaction volatiles were removed *in vacuo*, and the resulting red solid was crystallized from a minimal amount of pentane at −35 °C to afford 247 mg (0.314 mmol, 56%) of Ta(=NC^{t}Bu=CHC^{t}Bu=CH)(OAr)$_2$(THF) as red crystals. Anal. Calcd for $C_{40}H_{62}NO_3Ta$: C, 61.13; H, 7.95; N, 1.78. Found: C, 60.89; H, 7.96; N, 1.78.

Ta(=NC^{t}Bu=CHC^{t}Bu=CH)(OAr)$_2$(py)$_2$ (5·py). The bis(pyridine) adduct Ta(=NC^{t}Bu=CHC^{t}Bu=CH)(OAr)$_2$(py)$_2$ (**5**·py) is prepared in a manner analogous to that described above for Ta(=NC^{t}Bu=CHC^{t}Bu=CH)(OAr)$_2$(THF) (**5**·THF), except the recrystallization is carried out in pentane with the addition of several drops of pyridine. This procedure affords **5**·py in 74% yield. Anal. Calcd for $C_{46}H_{64}N_3O_2Ta$: C, 63.36; H, 7.40; N, 4.82. Found: C, 62.98; H, 7.63; N, 4.54.

[Ta(μ-NC^{t}Bu=CHC^{t}Bu=CH)(OAr)$_2$]$_2$ (6). Ta(=NC^{t}Bu=CHC^{t}Bu=CH)(OAr)$_2$(THF) (**5**·THF) (32 mg, 0.041 mmol) was dissolved in 0.5 mL of C_6D_6, trimethylsilyl iodide (5.8 μL, 0.041 mmol) was added neat, and the red solution was sealed in a 5-mm NMR tube. The solution was heated at 80 °C for 12 h, over which time large, well-formed, insoluble red crystals formed at the bottom of the tube. The solution was cooled to room temperature, and ^{1}H NMR examination of the nearly decolorized solution showed the complete disappearance of resonances attributable to Ta(=NC^{t}Bu=CHC^{t}Bu=CH)(OAr)$_2$(THF) (**5**·THF) and the appearance of resonances due to the formation of $Me_3SiOCH_2CH_2CH_2CH_2I$.[14] The tube was broken open, and the crystals were collected by filtration and dried *in vacuo*. The identity of these crystals as [Ta(μ-NC^{t}Bu=CHC^{t}Bu=CH)(OAr)$_2$]$_2$ (**6**) was confirmed by a comparison of one crystal's unit cell parameters to those of an authentic sample of **6**.[8] Anal. Calcd for $C_{72}H_{108}N_2O_4Ta_2$: C, 60.58; H, 7.63; N, 1.96. Found: C, 60.81; H, 7.82; N, 1.94.

(17) Choi, J.-G.; Brenner, J. R.; Colling, C. W.; Demczyk, B. G.; Dunning, J. L.; Thompson, L. T. *Catal. Today* **1992**, *15*, 201.
(18) Kleckley, T. S.; Bennett, J. L.; Wolczanski, P. T.; Lobkovsky, E. B. *J. Am. Chem. Soc.* **1997**, *119*, 247.
(19) Bonanno, J. B.; Henry, T. P.; Neithamer, D. R.; Wolczanski, P. T.; Lobkovsky, E. B. *J. Am. Chem. Soc.* **1996**, *118*, 5132.
(20) Durfee, L. D.; Fanwick, P. E.; Rothwell, I. P.; Folting, K.; Huffman, J. C. *J. Am. Chem. Soc.* **1987**, *109*, 4720.
(21) Mayer, J. M.; Curtis, C. J.; Bercaw, J. E. *J. Am. Chem. Soc.* **1983**, *105*, 2651.
(22) Shriver, D. F.; Drezdzon, M. A. *The Manipulation of Air-Sensitive Compounds*, 2nd ed.; John Wiley and Sons: New York, 1986.
(23) Perrin, D. D.; Armarego, W. L. F. *Purification of Laboratory Chemicals*, 3rd ed.; Pergamon Press: Oxford, 1988.

Ta[=NC^{t}Bu=CHC^{t}Bu=CHC(=N^{t}Bu)O](OAr)$_2$ (7). Ta(=NC^{t}Bu=CHC^{t}Bu=CH)(OAr)$_2$(THF) (**5**·THF) (200 mg, 0.255 mmol) was dissolved in 10 mL of C_6H_6, and neat ^{t}BuNCO (30 μL, 0.262 mmol) was added at room temperature. The solution color immediately changed from red to yellow. This mixture was stirred for 10 min, the reaction volatiles were removed *in vacuo*, and the resulting yellow solid was crystallized from toluene/pentane at −35 °C to afford 138 mg (0.170 mmol, 67%) of Ta[=NC^{t}Bu=CHC^{t}Bu=CHC(=N^{t}Bu)O](OAr)$_2$ as yellow crystals. IR (C_6H_6 solution, cm^{-1}): 3092 s, 3072 s, 3038 s, 2964 m, 2324 w, 2210 w, 1961 s, 1817 s, 1601 m, 1529 w, 1479 s, 1435 m, 1395 w, 1329 w, 1257 w, 1199 w, 1037 m, 908 w, 750 w, 675 s. Anal. Calcd for $C_{41}H_{63}N_2O_3Ta$: C, 60.58; H, 7.81; N, 3.45. Found: C, 60.56; H, 8.00; N, 3.20.

Ta[=NC^{t}Bu=CHC^{t}Bu=CH(η^3-C(=N^{i}Pr)$_2$)](OAr)$_2$ (8). Ta(=NC^{t}Bu=CHC^{t}Bu=CH)(OAr)$_2$(THF) (**5**·THF) (200 mg, 0.255 mmol) was dissolved in 10 mL of C_6H_6, and neat ^{i}PrNCN^{i}Pr (40 μL, 0.255 mmol) was added at room temperature. The solution color immediately changed from red to yellow. This mixture was stirred for 5 min; the reaction volatiles were removed *in vacuo* to afford a yellow oil. This oil was dissolved in pentane and the solvent removed *in vacuo* to form a yellow solid that was crystallized from pentane at −35 °C to provide 130 mg (0.155 mmol, 61%) of Ta[=NC^{t}Bu=CHC^{t}Bu=CH(η^3-C(=N^{i}Pr)$_2$)](OAr)$_2$. IR (C_6H_6 solution, cm^{-1}): 3080 s, 3071 s, 3036 s, 2963 w, 2359 m, 2324 m, 1961 s, 1817 s, 1529 w, 1479 s, 1435 w, 1394 w, 1332 w, 1259 w, 1207 w, 1037 s, 671 s. Anal. Calcd for $C_{43}H_{68}N_3O_2Ta$: C, 61.49; H, 8.16; N, 5.00. Found: C, 61.84; H, 8.46; N, 4.76.

X-ray Structural Determination of Ta(=NC^{t}Bu=CHC^{t}Bu=CH)(OAr)$_2$(THF) (5·THF). An orange, thin, plate crystal of $C_{40}H_{62}NO_3Ta$ was crystallized from concentrated pentane solution (−35 °C) and was mounted on a glass fiber in a random orientation. There were no systematic absences; the space group was determined to be *P*1 (No. 2). Hydrogen atoms were not located but were added at calculated positions; subsequently they were included in the structure factor calculations, but their positions were not refined. Scattering factors were taken from Cromer and Waber.[24] Anomalous dispersion effects were included in F_c.[25] The values for $\Delta f'$ and $\Delta f''$ were those of Cromer.[26] All calculations were performed on a VAX computer using MolEN.[27] Details of the structural determination and refinement are reported in Table 4.

Acknowledgment. Thanks is given to the Division of Chemical Sciences, Office of Basic Energy Sciences, Office of Energy Research, U.S. Department of Energy (DE-FG03-93ER14349), for support of this research.

Supporting Information Available: Complete crystallographic details, including tables of atomic positional and thermal parameters, bond distances and angles, least-squares planes, dihedral angles, and ORTEP figures for Ta(=NC^{t}Bu=CHC^{t}Bu=CH)(OAr)$_2$(THF) (**5**·THF) (27 pages). Ordering information is given on any current masthead page.

OM970749R

(24) Cromer, D. T.; Waber, J. T. *International Tables for X-Ray Crystallography*; The Kynoch Press: Birmingham, England, 1974; Vol. IV, Table 2.2B.
(25) Ibers, J. A.; Hamilton, W. C. *Acta Crystallogr.* **1964**, *7*, 781.
(26) Cromer, D. T. *International Tables for X-Ray Crystallography*; The Kynoch Press: Birmingham, England, 1974; Vol. IV, Table 2.3.1.
(27) *MolEN: An Interactive Structure Solution Procedure*; Enraf-Nonius: Delft, The Netherlands, 1990.